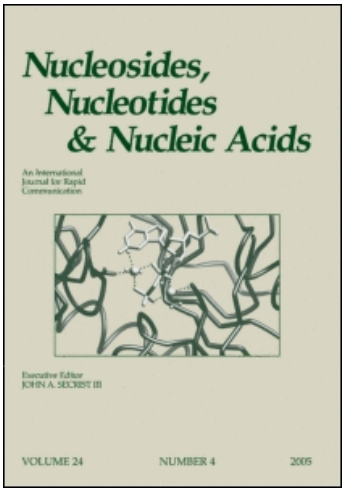

Nucleosides, Nucleotides and Nucleic Acids
Publication details, including instructions for authors and subscription information:
http://www.informaworld.com/smpp/title~content=t713597286

Biodistribution and Imaging of 1-(2-Deoxy-β-D-Ribofuranosyl)-2,4-Difluoro-5-[$^{123/125}$I]Iodobenzene (dRF[$^{123/125}$I]IB), A Nonpolar Thymidine-Mimetic Nucleoside, in Rats and Tumor-Bearing Mice

Anke Stahlschmidt[a]; Panteha Khalili[b]; William Sun[bc]; Hans-Jürgen Machulla[a]; Edward E. Knaus[b]; Leonard I. Wiebe[bc]
[a] PET Center, Radiopharmacy, Eberhardt-Karls Universität Tübingen, Germany [b] Faculty of Pharmacy and Pharmaceutical Sciences, University of Alberta, Germany [c] PET Centre, Cross Cancer Institute, Edmonton, Canada

To cite this Article Stahlschmidt, Anke , Khalili, Panteha , Sun, William , Machulla, Hans-Jürgen , Knaus, Edward E. and Wiebe, Leonard I.(2009) 'Biodistribution and Imaging of 1-(2-Deoxy-β-D-Ribofuranosyl)-2,4-Difluoro-5-[$^{123/125}$I]Iodobenzene (dRF[$^{123/125}$I]IB), A Nonpolar Thymidine-Mimetic Nucleoside, in Rats and Tumor-Bearing Mice', Nucleosides, Nucleotides and Nucleic Acids, 28: 5, 379 — 393
To link to this Article: DOI: 10.1080/15257770903051072
URL: http://dx.doi.org/10.1080/15257770903051072

Nucleosides, Nucleotides and Nucleic Acids, 28:379–393, 2009

ISSN: 1525-7770 print / 1532-2335 online
DOI: 10.1080/15257770903051072

Taylor & Francis
Taylor & Francis Group

BIODISTRIBUTION AND IMAGING OF 1-(2-DEOXY-β-D-RIBOFURANOSYL)-2,4-DIFLUORO-5-[$^{123/125}$I]IODOBENZENE (dRF[$^{123/125}$I]IB), A NONPOLAR THYMIDINE-MIMETIC NUCLEOSIDE, IN RATS AND TUMOR-BEARING MICE

Anke Stahlschmidt,[1] Panteha Khalili,[2] William Sun,[2,3] Hans-Jürgen Machulla,[1] Edward E. Knaus,[2] and Leonard I. Wiebe[2,3]

[1]*PET Center, Radiopharmacy, Eberhardt-Karls Universität Tübingen, Germany*
[2]*Faculty of Pharmacy and Pharmaceutical Sciences, University of Alberta, Germany*
[3]*PET Centre, Cross Cancer Institute, Edmonton, Canada*

□ *1-(2-Deoxy-β-D-ribofuranosyl)-2,4-difluoro-5-iodobenzene (dRFIB) is a putative bioisostere of iododeoxyuridine (IUdR). The advantages of dRFIB over IUdR for in vivo studies include resistance to both phosphorolytic cleavage of the nucleoside bond and de-iodination. dRFIB was radioiodinated (dRF$^{123/125}$IB) by copper-catalyzed exchange using commercial sodium [$^{123/125}$I]iodide. The in vivo biodistribution of dRF[^{125}I]IB in BALBc mice and imaging of dRF[^{123}I]IB in Sprague-Dawley rats are reported. In vivo data for rats show rapid clearance of radioactivity from blood (> 95%ID in 15 minutes), extensive excretion in urine (56%ID/24 hours), concentration in the hepatobiliary-small intestine system and very little fecal excretion (∼3%ID/24 hours). Pharmacokinetic data for dRF[^{125}I]IB (i.v. 48.7 ug/kg) in rats ($t_{1/2}$[h] = 0.51 ± 0.14, AUC_{inf}[μg.min/mL] = 3.7 ± 0.4, Cl[L/kg/h] = 0.75 ± 0.12, Vss[L/kg] = 0.96 ± 0.18) confirm previously reported dose-dependent pharmacokinetics. Scintigraphic images of rats dosed with dRF[^{123}I]I were compatible with rapid soft-tissue clearance and extensive accumulation of radioactivity in bladder/urine and liver/small intestine. In tumor-bearing mice, thyroid and stomach radioactivity was indicative of moderate deiodination. An unidentified polar radioactive metabolite was detected in serum.*

Received 10 December 2008; accepted 19 March 2009.
This article is published as part of the Morris J. Robins 70th birthday issue.
The authors wish to thank Dr. Douglas Abrams and Mr. Dwayne Rakowski, Edmonton Radiopharmacy Centre, for assisting with the imaging protocols; Dr. Terrance Riauka, Cross Cancer Institute, for assistance with processing the gamma camera images; Mr. Hans-Jörg Rahm, Tübingen University, for assistance with graphics; and Ms. Jennifer Yang for reviewing the kinetic analyses. L.I.W. was the recipient of an Alexander von Humboldt fellowship during part of this work. This project was carried out with partial support from the Canadian Institutes of Health Research (CIHR grant 14480).
Address correspondence to Leonard I Wiebe, 1807 Cross Cancer Institute, 11560 University Ave, Edmonton T6G 1Z2, Canada. E-mail: Leonard.wiebe@ualberta.ca

Keywords Thymidine mimic; difluorophenyl deoxyribosides; dRF[$^{123/125}$I]IB; biodistribution and pharmacokinetics; scintigraphic imaging; thymidine kinase; nucleoside transport

INTRODUCTION

Single photon emission computed tomography (SPECT) and positron emission tomography (PET) are invaluable imaging-based techniques for the early diagnosis of cancer and for cancer treatment planning and monitoring. Specific objectives of nucleoside-based imaging include monitoring tumor cell proliferation and imaging the expression of Herpes simplex type-1 thymidine kinase (HSV-TK) after HSV-*tk* transgene gene therapy. Thus, metabolic trapping of radiolabelled nucleosides that are substrates for mammalian thymidine kinase-1 (TK1) reflects cell proliferation on the principle that TK expression correlates with the number of cells in the S-phase of the cell cycle,[1] that is, accumulation of TK substrate radioactivity in a region/tissue of interest mirrors cell cycling in that region. Many nucleosides labelled with gamma- or positron-emitting radionuclides have been proposed and used for cell proliferation imaging, including ^{11}C-thymidine (^{11}C-TdR)[2] and 5-[^{18}F]fluoro-2′-deoxyuridine ([^{18}F]FUdR).[3] ^{11}C-TdR was the first nucleoside to be used clinically for oncological PET imaging.[4] Today, 3′-[^{18}F]fluoro-3′-deoxythymidine (FLT) is the most commonly used radiopharmaceutical for cell proliferation assessments in clinical oncology. FLT is a good thymidine kinase substrate and at the same time offers the advantage of resistance to phosphorolytic cleavage of the nucleoside bond, which reduces the number of metabolites and thereby simplifies image analysis and interpretation.[5–7] Radioiodinated nucleosides used for image-based monitoring of HSV-TK expression in herpesvirus infections[8–10] and for HSV-1 TK based transgene expression studies[11–14] must be a substrates for HSV-1 TK, but not for mammalian TK1. The design of radiolabelled nucleosides for imaging-based cell proliferation and viral TK-expression monitoring,[15,16] and clinical and preclinical applications of HSV-TK based transgene imaging[17,18] are the subject of numerous reviews.

Synthetic *C*-nucleosides represent one approach to designing better diagnostic and therapeutic nucleosides. Early interest in *C*-nucleosides was based on pseudouridine (ψ-uridine), a natural product[19] occurring ubiquitously as a minor component in various tRNAs. Chemically, the ψ-uridines are comprised of a uracil base coupled via C-5 to the ribosyl moiety. Although these compounds are essentially devoid of biological activity (ψ-isocytidine has growth inhibitory effects[20]), some, like 2′-deoxy-l-methyl-ψ-uridine (ψ-thymidine; a *C*-nucleoside analogue of thymidine;[21] Figure 1), have been utilized to develop strategies to expand the genetic

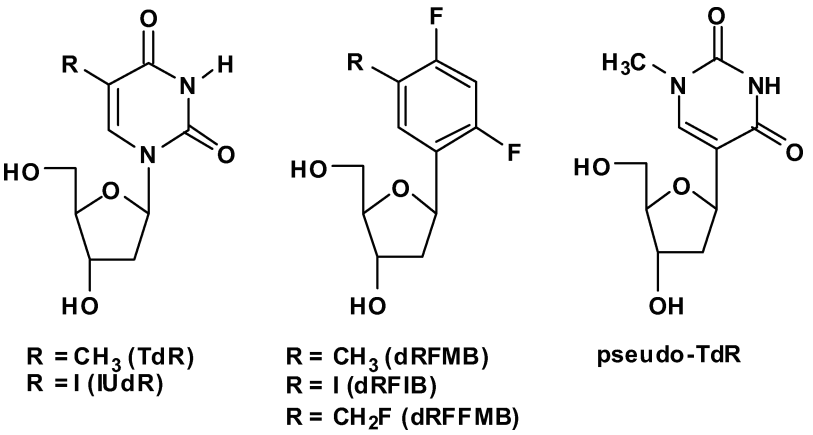

FIGURE 1 Chemical structures of the pyrimidine nucleosides thymidine (TdR) and iododeoxyuridine (IUdR), and the difluorophenyl deoxyriboside thymidine mimics, dRFMB, dRFIB and dRFFMB, and pseudothymidine (pseudo-TdR).

alphabet.[22] A study of the metabolism of radiolabeled ψ-thymidine in mice demonstrated that this *C*-nucleoside is not hydrolyzed, but also failed to find evidence that it was utilized metabolically in vivo.[23]

Other novel *C*-nucleoside thymidine analogues include those in which a difluorophenyl 'nucleobase' is coupled to deoxyribose to form nonpolar, lipophilic nucleoside mimics[24,25] that are phosphorylase resistant[26] in comparison to TdR and other natural nucleosides which undergo rapid degradation in blood.[27] When triphosphorylated, these novel *C*-nucleosides, in which thymine is replaced by a bioisosteric 5-methyl-2,4-difluorophenyl moiety (Figure 1), are inserted into DNA opposite adenine with high fidelity and undergo efficient incorporation into DNA fragments.[28] 1-(2-Deoxy-β-D-ribofuranosyl)-2,4-difluoro-5-iodobenzene (dRFIB), a bioisostere of iododeoxyuridine (IUdR; Figure 1), is a weak TK substrate; its phosphorylation rate is only 10% of TdR, and its phosphorylation is competitively inhibited by TdR.[29] Dose-dependent pharmacokinetics of dRFIB at high doses have been reported, with more rapid clearance and increased urinary excretion as doses decreased from 55 mg/kg to 5 mg/kg. Unchanged dRFIB and dRFIB-glucuronides are excreted in urine.[26,30] A second difluorophenyl nucleoside, 1-(2-deoxy-β-D-ribofuranosyl)-2,4-difluoro-5-[^{18}F]fluoromethylbenzene (dRFFMB), putatively bioisosteric to FUdR or TdR, has been reported to undergo rapid defluorination in vivo.[31] The potential of these *C*-nucleoside thymidine mimics for use as cell proliferation imaging agents is therefore uncertain.

To further expand the knowledge base for this class of thymidine mimics, preliminary pharmacokinetic data for radioiodinated dRFIB at radiotracer doses of $\sim$50 μg/kg in rats are now reported, together with

scintigraphic images in rats and whole-body biodistribution data in tumor-bearing mice.

EXPERIMENTAL

Radiolabelling

1-(2-Deoxy-ß-D-ribofuranosyl-2,4-difluoro-5-[$^{123/125}$I]iodobenzene (dRF$^{123/125}$IB) was radiolabelled with either [^{123}I]iodide or [^{125}I]iodide via isotope exchange as described elsewhere.[32] In a typical reaction, the precursor (dRFIB; ~1 mg) was dissolved in methanol (1 mL), and an aliquot (100 μL; ~100 μg dRFIB) was added to aqueous $CuSO_4$ solution (0.36 mM; 100 μL) mixed with aqueous $(NH_4)_2SO_4$ buffer (3.6 mM; 100 μL). [^{123}I]Iodide (40 MBq in 20 μL 0.1 M NaOH) was added, then the reaction vial was closed, a syringe filled with activated carbon to trap volatile radioiodine was attached for ventilation, and then the vial was heated at 120°C for 1 hour. The resulting solution was passed through a C-18 cartridge pre-activated with methanol (10 mL) and washed with water (10 mL). Following a water flush (10 mL), elution with methanol (4 mL) afforded the labelled product (dRF[$^{123/125}$I]IB) with radiochemical purity >98% by radio-HPLC assay.

Animals were handled in accordance with guidelines established by the Canadian Council of Animal Care. All experimental and surgical protocols were approved by the University of Alberta Health Sciences Animal Welfare Committee.

Pharmacokinetics

Adult male Sprague Dawley rats (250 g; Health Sciences Laboratory Animal Services, University of Alberta) were fitted with an indwelling jugular vein cannula 1 day before intravenous (i.v.) dosing with dRF[^{125}I]IB (46.8 μg/kg). The animals were dosed via the catheter. After injection via the catheter, it was flushed in situ with blood (150 μL, previously taken from the rat) and then with saline (300 μL) to avoid contamination of subsequent blood samples taken via this catheter.[33] Blood samples (250 μL) from the first animal were withdrawn 1, 5, 10, 15, 30, 45, 60, 90, 120, 150, and 180 minutes after injection, to establish appropriate sampling times. On this basis, samples were withdrawn 1, 3, 5, 7, 10, 15, 30, 45, 60, 90, 120, 180, and 1440 minutes after injection. The catheter was flushed with saline (300 μL) after each withdrawal to clear residual blood and radioactivity, and to maintain hydration of the animal. Blood samples were stored on ice prior to work up. Aliquots (50 μL) of each blood sample were radioassayed (total radioactivity) and larger aliquots (200 μL) were added to ice-cold acetonitrile (650 μL) to precipitate proteins and macromolecules. The

latter samples were centrifuged and the supernatant was filtered through a 0.45 μm syringe filter. Aliquots of the resulting serum filtrates (50 μL) were taken for radioassay, and second aliquots (100 μL) of serum were analyzed by HPLC. Urine and feces of rats housed in metabolic cages were collected for 24 hours and radioassayed. The volume of collected urine was measured; three aliquots (50 μL each) were taken for radioassay and two aliquots (25 μL each) were subjected to HPLC analysis. Pharmacokinetic parameters were estimated from blood radioactivity data using an industry standard pharmacokinetics package (WinNonlin version 1.1; Pharsight Corporation, USA).

Imaging

dRF[^{123}I]IB was injected into two rats via their tail veins. One rat (250 g) received 3.9 MBq of dRF[^{123}I]IB (11.7 μg; 107 MBq/μmol), the second rat (600 g) received a dose of 3.6 MBq. The rats were immobilized under light isoflurane anesthesia during imaging. A dynamic scan (Siemens Orbiter Digitrac 3700, LEAP//PH collimator, Odyssey FX Image software, V8.5.6 3/28/99 processor) was performed over the first 20 minutes (32 frames/30 sec) and static images (20 minutes acquisitions) were acquired after 30, 70, 100 and 130 minutes for the 250 g rat and 30, 60, 90, and 120 minutes for larger rat.

Biodistribution

EMT6 tumor cells in suspension were injected subcutaneously under the left front leg of male Balb/C mice (20–24 g; Health Sciences Laboratory Animal Services, University of Alberta). After the tumors grew to an appropriate size (0.7–1 cc as estimated by calliper measurement), dRF[^{125}I]IB (46.8 μg/kg) was injected via the tail vein. At preselected times after dosing, the mice (n = 3 per time point) were euthanized, tissues and/or organs were removed by dissection, and their weights were recorded prior to radioassay.

Blood and Urine Analysis

Total radioactivity per aliquot was determined by counting using a well-type gamma scintillation counter. HPLC analyses were carried out on a reverse phase Radial-Pak cartridge column (8NVC184μ, Nova-Pak, C-18; Waters, Canada) with a guard column of the same material, using acetonitrile:water 45:55 v/v at a flow of 1 mL/min. The retention time for authentic dRFIB was 12.5 minutes; iodide eluted as a broad peak just before dRFIB. Eluant fractions corresponding to UV absorption peaks (273 nm) were collected for radiometry.

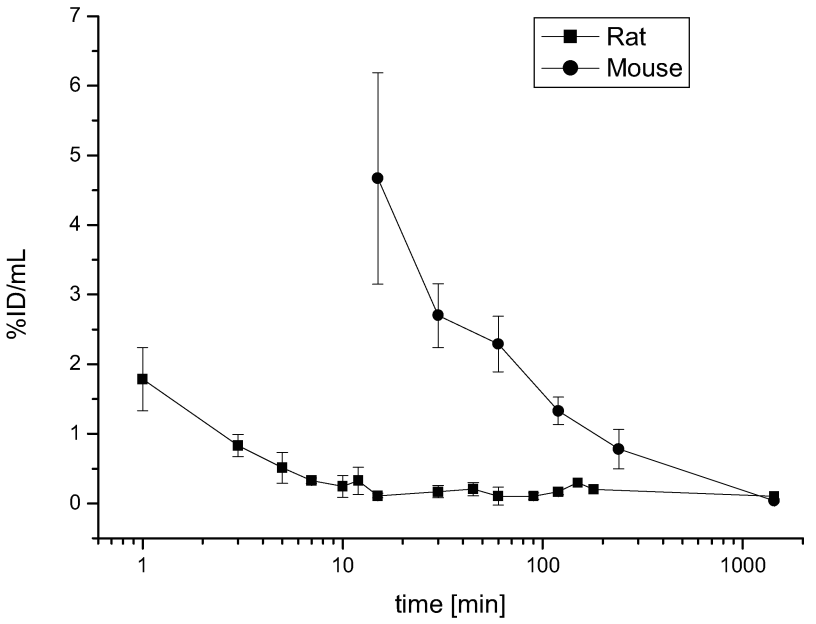

FIGURE 2 Clearance of radioactivity from blood, after bolus i.v. injection of dRF[^{125}I]IB, as a function of time, in rats (■) and mice (●). Data are means, n = 3 ± S.D.

RESULTS

The amount of radioactivity of dRF[^{125}I]IB in rat blood decreased rapidly over the first 5 minutes following injection, to <1% of the injected dose (%ID). About 56% of the administered radioactivity was recovered in urine over 24 hours, and another 3% of the injected dose was present in 0–24 hour faeces. The mean blood levels of dRF[^{125}I]IB, expressed as a percentage of injected dose/mL (%ID/mL), are plotted in Figure 2 as a function of time after injection.

Blood samples were analyzed by radio-HPLC to quantify unchanged dRF[^{125}I]IB as a percentage of total radioactivity. These data, presented as %ID/mL blood in Figure 3, show that unchanged dRF[^{125}I]IB, as a fraction of total blood radioactivity, decreased rapidly in the first hour, from approximately 87% down to 11%, then increased at late intervals (24 hours) to the fractional content present in the early fractions. That is, dRF[^{125}I]IB in the last fraction accounted for 78% of the total radioactivity in this blood sample. This effect may be due to hepatobiliary recirculation, as postulated for high dose dRFIB (53.4 mg/kg).[26] The radioactive metabolites observed as HPLC peaks in the chromatograms were all more polar than dRF[^{125}I]I as indicated by their shorter retention times. Two radioactive metabolites were found, but not unequivocally identified; one was thought to be radioiodide,

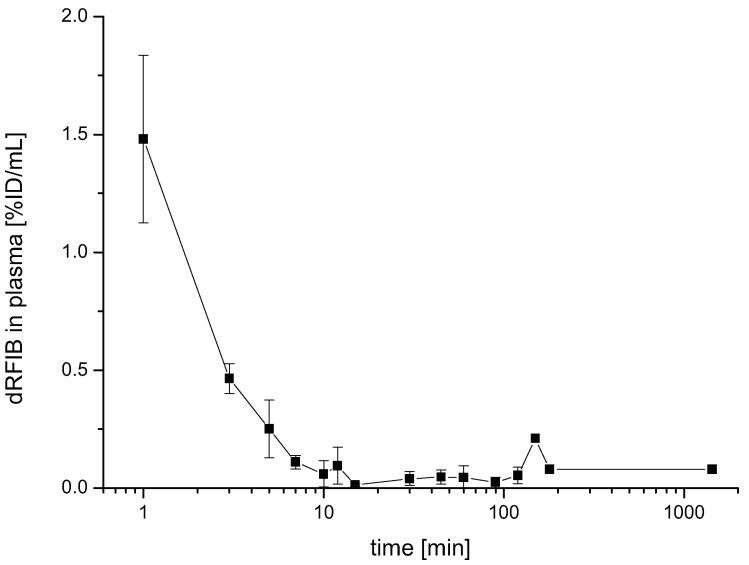

FIGURE 3 dRF[^{125}I]IB as%ID/mL in rat blood after i.v. injection of dRF[^{125}I]IB via a catheter. Data are means, n = 3 ± S.D.

based on HPLC elution volume. An in vitro study incubation in blood showed about 7% deiodination.

Analysis of the total radioactivity data (Figure 2) provided an elimination half-life ($t_{1/2}$ = 0.51 hours) that was relatively long compared to the $t_{1/2}$ at higher doses; the distribution volume (Vss = 0.96 ± 0.18 L/kg) was greater than the average total body water in rats, and clearance (Cl = 0.75 ± 0.12 L/kg/h) was low at this tracer dose compared with literature data for much larger doses of the unlabelled compound.[26] Pharmacokinetic analysis of dRF[^{125}I]IB data in the rat indicated a very short distribution half-life (0.04 hours), a large distribution volume (~50 L/kg) and high clearance (~20 L/kg/h), but these values are only rough approximations at best, since the raw data could not be accurately modelled.

For both total radioactivity and dRF[^{125}I]IB data, the large volumes of distribution imply rapid and extensive intracellular distribution and are compatible with the very rapid distribution phase observed. Literature data for dRFIB are based on doses up to 53.6 mg/kg, about three orders of magnitude greater than the dose used in this study (48.7 μg/kg), provide an insight into the impact of dose on distribution kinetics. Selected pharmacokinetic data from the literature and from this study are summarized in Table 1.

Literature data for the intermediate doses (5 and 15 mg/kg) were obtained using a two-compartment model, whereas the data for the radioactive compound and 53.6 mg/kg dose were modelled using a noncompartmental model. Data obtained for the radioactive compound (low dose dRF[^{125}I]IB)

TABLE 1 Pharmacokinetic data for single intravenous doses of dRFIB[21,25] and tracer kinetics for dRF[^{125}I]IB, in rats (n = 3 ± SD)

PK Parameter	Rat Total ^{125}I 48.7 ug/kg	Rat dRFIB[30] 5 mg/kg	Rat dRFIB[30] 15 mg/kg	Rat dRFIB[26] 53.6 mg/kg
$t_{1/2}$ [h]	0.51 ± 0.14	0.14 ± 0.01	0.13 ± 0.01	0.35 ± 0.27
AUC_{inf} [μg.min/mL]	3.70 ± 0.40	174 ± 10	472 ± 60	2872 ± 149
Cl [L/kg/h]	0.75 ± 0.12	1.72 ± 0.06	1.93 ± 0.23	1.23 ± 0.17
Vss [L/kg]	0.96 ± 0.18	0.30 ± 0.03	0.33 ± 0.02	0.38 ± 0.06

could not be modeled satisfactorily due to the very rapid early clearance and undulating blood levels.

Blood level data (Figure 2) for dRF[^{125}I]IB in mice show more gradual clearance than for rats, with 5% ID/g in blood after 15 minutes and 1%ID/g after 2 hours. After 24 hours, concentrations in blood were virtually identical in rats and mice. Accumulation of radioactivity in tumor reached a maximum of approximately 5% ID/g after 1 hour, with the highest tumor:blood ratio (3.5) occurring 2 hours after dosing. The relatively small amounts of radioactivity in 0–24 hours feces, when combined with gut, liver, and bile data, support a model of hepatic uptake and metabolic degradation leading predominantly to water-soluble metabolites which are excreted in the urine (56%ID in total over 24 hours). Liver, thyroid, and tumor radioactivity levels increased during the first hour following injection, whereas other tissues like lung, kidney, and tail (injection site) essentially followed blood level changes (Figure 4). Total thyroid radioactivity levels were approximately 5%ID between 15 and 240 minutes, and dropped to <1%ID after 24 hours. Deiodination in vivo, based on combined thyroid and stomach radioactivity, represented approximately 15% of the injected dose in mice (Figure 4), in line with the deiodination observed during an incubation of dRF[^{125}I]IB in fresh whole blood in vitro (~7%). Biodistribution data, expressed as%ID per whole organ are provided in Figure 4.

Two static images obtained for rat #1 (weight 250 g) are shown in Figure 5. Tissue perfusion by dRF[^{125}I]IB was evident in the dynamic scan (images not shown). Uptake by the liver and accumulation in the intestine, visible almost from the start of imaging, was indicative of hepatobiliary clearance. The first static image (70 minutes; Figure 5, right side image) showed accumulation in the stomach and thyroid (deiodination), bladder (renal clearance) and intestine, as well as major blood vessels and heart (blood radioactivity). In later static images (130 minutes; Figure 4) the background radioactivity decreased, while radioactivity accumulation in stomach and thyroid increased. Radioactivity in the bladder was high throughout, whereas it was low-moderate in the thyroid during the entire imaging procedure. In contrast to the biodistribution study in mice, region

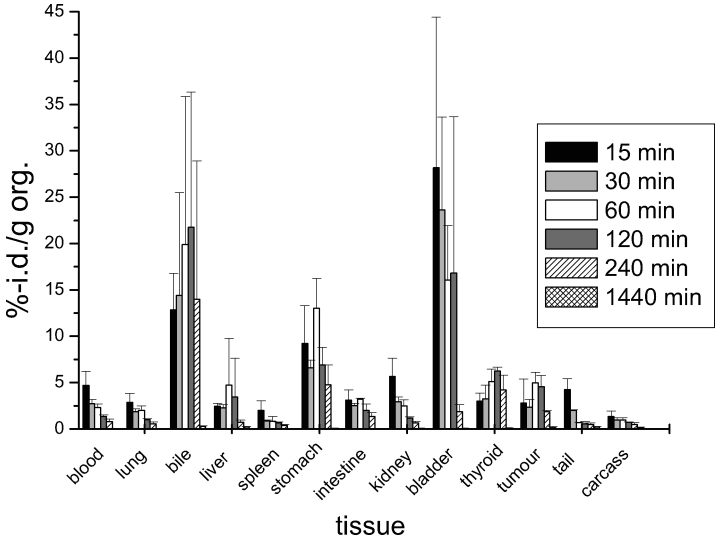

FIGURE 4 Biodistribution of dRF[^{125}I]IB (46.8 μg/kg) in mice after i.v. bolus into tail vein. Data are mean%ID/organ values, n = 3 ± S.D.

of interest measurements (rat images) revealed slight increases in thyroid towards the end of the imaging procedure. Although the dose/g to the second rat was only 40% of that to the first rat, and although the second rat was much larger and older, only minor qualitative differences were observed in the images of these two animals, mainly showing much less renal/bladder radioactivity in the larger rat (not shown).

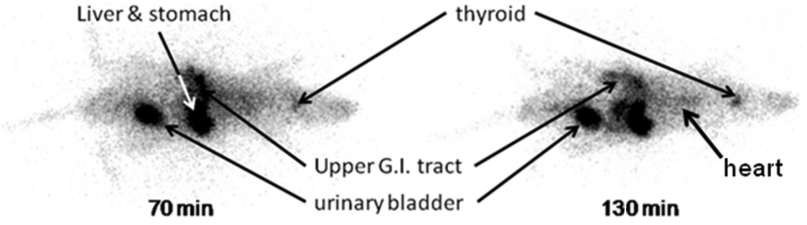

FIGURE 5 Static scintigraphic images of a rat (250 g), dosed with 3.9 MBq of dRF[^{123}I]IB via bolus tail vein injection. The images were taken 70 (left) and 130 (right) minutes after injection under isoflurane anaesthesia. Acquisition time was 20 minutes per image. Both images depict radioactivity in bladder, liver-intestine-stomach and thyroid in addition to generalized low-level radioactivity. Radioactivity in blood appears to be provide above background image density in the region of the heart and aorta, and an outline of the entire animal. Since dRF[^{123}I]IB is very lipophilic, and given the rapid clearance from blood in the rat (Figure 2), nonspecific partitioning from blood into soft tissues may also explain the general high background observed.

DISCUSSION

Substantial in vitro biochemical DNA-level interaction of dRFMB as a thymidine mimic has been reported.[28] A second member of this class of thymidine mimics, dRFIB, has been reported to exhibit pyrimidine nucleoside-like properties at the cellular level, as both a cell membrane permeant through interaction with the human concentrative nucleoside transporter 1 (hCNT1)[34] and as a relatively weak substrate for phosphorylation by nucleoside kinases.[29] Whole-body pharmacokinetic and metabolic studies at high doses pointed to rapid blood clearance, substantial hepatobiliary recycling with extensive renal elimination, dose-dependent pharmacokinetics and minimal deiodination.[26,30]

The current biological evaluation of low radiotracer doses of dRF[^{125}I]IB in rats showed rapid clearance from blood, with serum levels of dRF[^{125}I]IB decreasing after i.v. bolus injection to a level below 1% of the injected dose within the first 5 minutes (Figure 2). This rapid distribution phase is to be expected given the small chemical dose (47 μg/kg) and the high lipophilicity of dRF[^{125}I]IB. High lipophilicity contributes to rapid extravasation and dissociation into lipoidal tissues. As shown by the pharmacokinetic analysis (Table 1) this gives rise to the relatively large biodistribution volume (Vss = 0.96 ± 0.18 L/kg) observed. Once this fast distribution phase is complete (<5 minutes), the model changes completely, that is, protracted blood clearance (Cl = 0.75 ± 0.12 L/kg/h) of the remaining traces of radioactivity as anticipated for a compound that is highly protein bound. However, the pharmacokinetic model is complicated by periodic increases in the concentration of total radioactivity and dRF[^{125}I]IB in blood. Comparative pharmacokinetic data are not available for ψ-thymidine, but it appears that in contrast to dRF[^{125}I]IB, it is not cleared from blood, with between ~4 and ~6% of ID in blood at times of 5–240 minutes after injection.[23] These differences in the distribution phases may be due in part to their lipophilicity, since lipophilic compounds are known to partition rapidly from blood into lipoidal elements including fatty tissues and the phospholipid structures of cell membranes.[35] dRF[^{125}I]IB has a calculated partition coefficient (CLogP; Calculated using ChemDraw Ultra10, CambridgeSoft, USA) of 2.1534, about four orders of magnitude greater than ψ-thymidine (CLogP −2.5976) and two orders greater than IUdR (CLogP -0.4248). The CLogP values are derived from structural models and may vary somewhat from experimentally-derived values. For example, dRFIB has a CLogP of 2.1534, compared to a reported experimental value of 2.87.[26] Nonetheless, the CLogP values provide a good basis for the purposes of this work.

Just over half (56%ID) of the dose of radioactivity was present in urine collected over 24 hours, and analysis of the urine showed that only about 2% of this radioactivity was due to unchanged dRF[^{125}I]IB. Urinary metabolites

were not identified, but are likely to include glucuronide and sulphate conjugates, which were detected at higher doses.[30] A comparison of dRFIB literature data with the total radioactivity data obtained in this study shows that clearance decreased by one-third when the dose was reduced from 53.4 mg/kg to 46.8 μg/kg, and at the same time, the distribution volume increased by a factor of almost 3. The elimination half-life for the lower dose was higher by a factor of 3.4 compared to the higher dose. Unfortunately, pharmacokinetic analysis of dRF[^{125}I]IB data was not possible because of the complex, cyclic nature of changes in the concentration of dRF[^{125}I]IB in the blood as a function of time. By curtailing analysis at the 180 minutes interval, some pharmacokinetic estimates were possible, but poor fit precluded reliable estimation of statistical parameters. Total radioactivity data could be modeled, but these data reflect not only the nucleoside, but also radioactive metabolites.

In the earlier high dose studies, very little free dRFIB was found in bile; the hepatic capacity for glucuronidation over 8 hours was constant, between 150 and 200 μg, for doses ranging from 5 to 54 mg/kg, indicating saturated capacity at these doses. For the relatively small doses used in the current study, this glucuronidation capacity would be adequate to conjugate all of the dRFIB taken up by liver. These water-soluble metabolites (conjugates) would be renally cleared after re-entering the blood stream and thereby accounting for the high urinary excretion observed. In a competing pathway, the conjugates would be excreted in bile, hydrolyzed in the intestines and re-absorbed as the highly lipophilic (logP 2.87[26]) dRF[^{125}I]IB. The recycling pathway, together with re-distribution of dRF[^{125}I]IB from tissues back into the bloodstream, would account for the high fraction of dRF^{125}IB present in late serum samples, the low fecal excretion and the highly complex dRF[^{125}I]IB pharmacokinetics observed at the radiotracer dose.

Biodistribution studies with dRF[^{125}I]IB in tumor-bearing mice showed that most radioactivity was present in the bladder, bile, and stomach, further supporting a model of hepatobiliary recycling leading to the formation of water-soluble metabolites such as the glucuronide conjugates, and consequent renal elimination. The distribution phase and blood clearance in mice were slower than in the rat, but concentrations in blood reached corresponding rat levels within 24 hours (Figure 2). However, this prolonged distribution phase, with $\sim$1.5% ID in blood after 2 hours and $<$0.5% at 4 hours, is still very fast in comparison to radioiodinated iododeoxyuridine ([^{125}I]IUdR), which retained 11.2% of the injected dose in blood after 2 hours and 3.3% after 6 hours.[36] Biodistribution in mice was characterized by persistent stomach and thyroid radioactivity. The actual amounts in thyroid and stomach are indicative of deiodination; quite surprisingly, thyroid retained about 5% of the ID throughout the study, similar to the values reported for [^{125}I]IUdR in the same animal/tumor

model.[36] Radioactivity levels in kidney, liver, and gut were consistent with the hepatobiliary recycling model evident in the rat. The retention of dRF[^{125}I]IB in tumor was low, peaking at ~5% ID at 1–2 hours, then dropping to half at 4 hours and to negligible levels at 24 hours. Tumor uptake was not investigated further, but given that dRF[^{125}I]IB is a poor substrate for mammalian thymidine kinases, and in line with the uptake and clearance data, it is postulated that a combination of decreased perfusion and concomitant slow back-diffusion account for this apparent uptake by tumor tissue. The tumor uptake of [^{125}I]IUdR, on the other hand, was steady at ~5% ID over the entire study period, indicative of metabolic trapping.[36]

The SPECT images obtained after administration of dRF[^{123}I]IB to rats represent preliminary experiments involving only two animals. The animals were anaesthetized during the imaging procedure, making it difficult to compare the kinetic information in these images with the data from pharmacokinetic studies, as the anaesthetic may alter the biodistribution in the imaging studies.[37] However, the levels of radioactivity in the intestines of both animals support the model of hepatobiliary metabolism. Radioactivity in the stomach and thyroid are indicative of moderate deiodination.

The moderate deiodination is in stark contrast to defluorination data for 1-(2-deoxy-β-D-ribofuranosyl)-2,4-difluoro-5-[^{18}F]fluoromethylbenzene (dRFFMB), which was rapidly and extensively defluorinated in vivo, yielding high radioactivity concentrations in bone.[31] 5-Fluoromethyl-, 5-difluoromethyl- and 5-trifluoromethyl-2′-deoxyuridines are known to undergo rapid defluorination under alkaline conditions[38–40] in which the electronegative properties of the uracil ring facilitate solvolysis of the fluoromethyl bond. A similar mechanism may be operative for the difluorophenyl moiety, possibly accounting for the facile defluorination of the fluoromethyl substituent of dRFFMB. In contrast, dRFIB is not readily deiodinated. The deiodination mechanism for IUdR and iodouracil, which readily undergo alkaline hydrolysis,[41] is quite different than the case for dRFIB, the former being a Michael system which facilitates C-5 dehalogenation by directing uracil-ring electrons to C-5, whereas the 5-iodo-difluorophenyl moiety is fully aromatic and therefore more resistant to cleavage of the C-I bond.

The active species responsible for the tissue radioactivity concentrations observed have not been identified, but dRFIB-monophosphate is an unlikely anabolite based on in vitro phosphorylation studies with TK1 and TK2.[29] The low potential for in vitro phosphorylation can be inferred from kcat/Km, the second order rate constant which indicates the catalytic efficiency of the enzyme; kcat is the first order rate constant, that is, the turnover number of the enzyme, which defines the maximum number of substrate molecules converted to product per unit of time (s^{-1}), and Km represents the substrate concentration ([S]; μM) at half Vmax. kcat/Km

values for dRFIB were only 4% and 44% of TdR values for TK1 and TK2, respectively.[29] This low phosphorylation potential was not predictive of the apparent uptake of dRF[^{125}I]IB by tumor, but was compatible with the absence of appreciable uptake into bone marrow, where high phosphorylation reflects intensive cell cycling, seen in scintigraphic images of rats (Figure 5). High marrow uptake is expected for proliferation markers, and is observed in PET images using the proliferation marker FLT.[5]

SUMMARY

dRFIB demonstrated complex pharmacokinetics at radiotracer doses. Rapid blood clearance with persistent and even increasing levels of dRFIB in late blood samples, extensive urinary excretion, and minimal fecal excretion support a model of extensive hepatobiliary recycling with minimal deiodination. Although these observations appear to preclude a future for dRFIB as a cell proliferation imaging agent, additional studies are required to further ascertain its potential to function as a marker for cellular expression of a *tk*-transgene, for example, as a substrate of herpes simplex type-1 thymidine kinase (HSV-1 TK).

ABBREVIATIONS

dRFIB	1-(2-deoxy-β-D-ribofuranosyl)-2,4-difluoro-5-iodobenzene
dRFFMB	1-(2-deoxy-β-D-ribofuranosyl)-2,4-difluoro-5-[^{18}F]fluoromethylbenzene
dRFMB	1-(2-deoxy-β-D-ribofuranosyl)-2,4-difluoro-5-methylbenzene
TdR	thymidine
IUdR	iododeoxyuridine
hCNT1	human concentrative nucleoside transporter 1
HSV-1 TK	herpes simplex type-1 thymidine kinase
TK	mammalian thymidine kinase type-1
%ID	percentage of the injected dose

REFERENCES

1. Kornberg, A.; Baker, T.A., eds. Biosynthesis of DNA precursors, in *DNA Replication 2nd Ed.*, Freeman, W.H., New York, **1992**, pp. 53–100.
2. Christman, D.; Crawford, E.J.; Friedkin, M.; Wolf, A.P. Detection of DNA synthesis in intact organisms with positron-emitting [methyl-11C]thymidine. *Proc. Nat. Acad. Sci. USA*, **1972**, 988–992.
3. Abrams, D.N.; Knaus, EE, McQuarrie, S.A.; Wiebe, L.I. 18F-5-Fluoro-2′-deoxyuridine as a radiopharmaceutical for diagnostic oncology, in *The Chemistry of Radiopharmaceuticals*, eds. N.D. Heindel, H.D. Burns, T. Honda, and L.W. Brady, MASSON, New York, **1976**, pp. 205–213,
4. Martiat, P.; Ferrant, A.; Labar, D.; Cogneau, M.; Bol, A.; et al. In vivo measurement of carbon-11 thymidine uptake in non-Hodgkin's lymphoma using positron emission tomography. *J. Nucl. Med.* **1988**, 29, 1633–1637.
5. Shields, A.F.; Grierson, J.R.; Dohmen, B.M.; Machulla, H-J.; Stayanoff, J.C.; et al. Imaging proliferation in vivo with [F-18]FLT and positron emission tomography. *Nature Med.* **1998**, 4, 1334–1336.

6. Shields, A.; Lim, K.; Grierson, J.; Link, J.; Krohn, K.A. Utilization of labeled thymidine in DNA synthesis: studies for PET. *J. Nucl. Med.* **1990**, 31, 337–342.
7. Grierson, J.R.; Schwartz, J.L.; Muz, M.; Jordan, R.; Krohn, K.A. Metabolism of 3′-deoxy-3′-[F-18]fluorothymidine in proliferating A549 cells: validations for positron emission tomography. *Nucl. Med. Biol.* **2004**, 31, 829–837.
8. Samuel, J.; Knaus, E.E.; Wiebe, L.I.; Tyrrell, D.L. Synthesis of ^{131}I, ^{125}I and ^{82}Br labelled (E)-5-(2-halovinyl)-2′-deoxyuridines. *Int. J. Appl. Radiat. Isot.* **1984**, 35, 1049–1052.
9. Samuel, J. *Nucleosides for Herpes encephalitis diagnosis. Ph.D. thesis*, University of Alberta, 1985.
10. Tovell, D.R.; Samuel, J.; Mercer, J.R.; Misra, H.K.; Xu, L.; et al. The in vitro evaluation of nucleoside analogues as probes for use in the non-invasive diagnosis of Herpes Simplex encephalitis. *Drug Design Del.* **1988**, 3, 213–221.
11. Balzarini, J.; Morin, K.W.; Knaus, E.E.; Wiebe, L.I.; De Clercq, E. Novel (E)-5-(2-iodovinyl)-2′-deoxyuridine derivatives as potential cytostatic agents against Herpes Simplex Virus-thymidine kinase gene-transfected tumors. *Gene Ther.* **1995**, 2, 317–322.
12. Tjuvajev, J.G.; Stockhammer, G.; Desai, R.; Uehara, H.; Watanabe, K.; et al. Imaging the expression of transfected genes in vivo. *Cancer Res.* **1995**, 55, 6126–6132.
13. Morin, K.W.; Wiebe, L.I.; Knaus, E.E. Non-invasive scintigraphic monitoring of gene expression in a HSV-1 thymidine kinase gene therapy model. *Nucl. Med. Commun.* **1997**, 18, 599–605.
14. Haberkorn, U.; Mier, W.; Eisenhut, M. Scintigraphic imaging of gene expression and gene transfer. *Current Med. Chem.* **2005**, 12, 779–794.
15. Wiebe, L.I. Applications of nucleoside-based molecular probes for the in vivo assessment of tumour biochemistry using positron emission tomography (PET). *Brazil Arch. Biol. Technol.* **2007**, 50, 445–459.
16. Wiebe, L.I.; Morin, K.W.; Knaus, E.E. Radiopharmaceuticals to monitor gene transfer. *Quart. J. Nucl. Med.* **1997**, 41, 79–89.
17. Inubushi, M.; Tamaki, N. Radionuclide reporter gene imaging for cardiac gene therapy. *Eur. J. Nucl. Med. Mol. Imaging*, **2007**, 34(Suppl. 1), S27–S33.
18. Kuruppu, D.; Dorfman, J.D.; Tanabe, K.K. HSV-1 viral oncolysis and molecular imaging with PET. *Curr. Cancer Drug Targets* **2007**, 7, 175–180.
19. Cohn, W.E. Pseudouridine, a carbon-carbon linked ribonucleoside in ribonucleic acids: isolation, structure, and chemical characteristics. *J. Biol. Chem.* **1960**, 235, 1488–1498.
20. Chu, C.K.; Reichman, U.; Watanabe, K.A.; Fox, J.J. Nucleosides. CIX. 2′-Deoxy-Ψ-isocytidine, 2′-deoxy-Ψ-uridine, and 2′-deoxy-1-methyl-Ψ-uridine. Isosters of deoxycytidine, deoxyuridine and thymidine. *J. Heterocyclic Chem.* **1977**, 14, 1119–1121.
21. Matsuda, A.; Pankiewicz, K.; Marcus, B. K.; Watanabe, K. A.; Fox, J. J. Synthesis of 3-methylpseudouridine and 2′-deoxy-3-methylpseudouridine. *Carbohyd. Res.* **1982**, 100, 297–302.
22. Havemann, S.A.; Hoshika, S.; Hutter, D.; Benner, S.A. Incorporation of multiple sequential pseudothymidines by DNA polymerases and their impact on DNA Duplex Structure. *Nucleosides Nucleotides Nucleic Acids* **2008**, 27, 261–278.
23. Grierson, J.R.; Shields, A.F.; Zheng, M.; Kozawa, S.M.; Courter, J.H. Radiosyntheses of labeled pseudothymidine* ([C-11]- and [H-3 methyl) and its biodistribution and metabolism in normal and tumored mice. *Nucl. Med. Biol.* **1995**, 22, 671–678.
24. Schweitzer, B.A.; Kool, E.T. Aromatic nonpolar nucleosides as hydrophobic isosteres of pyrimidine and purine nucleosides. *J. Org. Chem.* **1994**, 59, 7238–7242.
25. Wang, Z-X.; Duan, W.; Wiebe, L.I.; Balzarini, J.; De Clercq, E.; Knaus, E.E. Synthesis of 1-(2-deoxy-b-D-ribofuranosyl)-2,4-difluoro-5-substituted-benzene thymidine mimics, some related a-anomers; and their evaluation as antiviral and anticancer agents. *Nucleosides Nucleotides Nucleic Acids* **2001**, 20, 11–40.
26. Khalili, P.; Naimi, E.; Knaus, E.E.; Wiebe, L.I. Pharmacokinetics and metabolism of the novel synthetic C-nucleoside, 1-(2-deoxy-b-D-ribofuranosyl)-2,4-difluoro-5-iodobenzene, a potential mimic of 5-iodo-2′-deoxyuridine. *Biopharm. Drug Dispos.* **2002**, 23, 105–113.
27. Shaw, T.; MacPhee, D.G. Rapid and complete degradation of thymidine by human peripheral blood platelets: implications for genotoxicity assays. *Mutation Res.* **1986**, 163, 75–80.
28. Kool, E.T.; Sintim, H.O. The difluorotoluene debate-a decade later. *Chem. Commun.* **2006**, 3665–3675.
29. Al-Madhoun, A.S.; Eriksson, S.; Wang, Z.X.; Naimi, E.; Knaus, E.E.; Wiebe, L.I. Phosphorylation of isocarbostyril- and difluorophenyl-nucleoside thymidine mimics by the human deoxynucleoside kinases. *Nucleosides Nucleotides Nucleic Acids* **2004**, 23, 1865–1874.

30. Khalili, P.; Naimi, E.; Sunm, W-Y., Knausm, E.E., Wiebe, L.I. Dose-dependent pharmacokinetics of 1-(2-deoxy-b-D-ribofuranosyl)-2,4-difluoro-5-iodobenzene: A potential mimic of 5-iodo-2′-deoxyuridine. *Biopharm. Drug Dispos.* **2003**, 24, 385–395.
31. Issa, W.; Tochon-Danguy, H.J.; Lambert, J.; Sachinidis, J.I.; Achermann, U.; et al. Synthesis and evaluation of a thymidine analogue for positron emission tomography study of tumor proliferation in vivo. *Nucl. Med. Biol.* **2004**, 31, 839–849.
32. Stahlschmidt, A.; Machulla, H-J.; Reischl, G.; Knaus, E.E.; Wiebe, L.I. Radioiodination of 1-(2-deoxy-b-D-ribofuranosyl)-2,4-difluoro-5-iodobenzene (dRFIB), a putative thymidine mimic nucleoside for cell proliferation studies. *Appl. Radiat. Isotopes* **2008**, 66, 1221–1228.
33. Stypinski, D.; Wiebe, L.I.; Mercer, J.R. A rapid and simple assay to determine the blood and urine concentrations of 1-(5-[^{123}/^{125}I]iodo-5-deoxyarabinofuranosyl)-2-nitroimidazole, a hypoxic cell marker. *J. Pharm. Biomed. Analysis* **1997**, 16, 1067–1073.
34. Smith, K.M.; Ng, A.M.L.; Yao, S.Y.M.; Labedz, K.A.; Knaus, E.E.; et al. Electrophysiological characterization of a recombinant human Na^+-coupled nucleoside transporter (hCNT1) produced in *Xenopus* oocytes. *J. Physiol. (Lond.)* **2004**, 558, 807–823.
35. Avdeef, A. Physicochemical profiling (solubility, permeability and charge state). *Curr. Top. Med. Chem.* **2001**, 1, 277–351.
36. Yang, X.-H.; Singh, S.; Kumar, P.; Diakur, J.; Wiebe, L.I. b-Cyclodextrin complexes of hydrolyzable adamantanoyl-IUdR prodrugs—radioiodination and biodistribution in mice bearing implanted KBALB tumours. *Current Radiopharmaceuticals* **2009**, 2, 137–142.
37. Stypinski, D.D.; Wiebe, L.I.; Tam, Y.K.; McEwan, A.J.B. Effects of methoxyflurane anesthesia on the pharmacokinetics of 125I-IAZA in Sprague-Dawley rats. *Nucl. Med. Biol.* **1999**, 26, 659–665.
38. Nestler, H.J.; Garrett, E.R. Prediction of stability in pharmaceutical preparations XV. Kinetics of hydrolysis of 5-trifluoromethyl-2′-deoxyuridine. *J. Pharm. Sci.* **1968**, 57, 1117–1124.
39. Tandon, M.; Kumar, P.; Wiebe, G.; Wiebe, L.I. Detection of new metabolites of trifluridine (F3TdR) using F NMR spectroscopy. *Biochem. Pharmac.* **1992**, 44, 2223–2228.
40. Tandon, M.; Kumar, P.; Wiebe, L.I. α-Trifluoromethyl-β-alanyl glycine (F_3MBAG): a novel mammalian metabolite of trifluridine (F3TdR). *Biochem. Pharmac.* **1994**, 48, 1033–1041.
41. Garrett, E.R.; Nestler, H.J.; Somodi, A. Kinetics and mechanisms of hydrolysis of 5-halouracils. *J. Org. Chem.* **1968**, 33, 3460–3468.